J Arid Land (2023) 15(9): 1052–1066
https://doi.org/10.1007/s40333-023-0106-4

Science Press Springer-Verlag

Environmental significance and hydrochemical characteristics of rivers in the western region of the Altay Mountains, China

LIU Shuangshuang[1,2], WANG Feiteng[1*], XU Chunhai[1], WANG Lin[1], LI Huilin[1]

[1] State Key Laboratory of Cryospheric Science, Northwest Institute of Eco-Environment and Resources, Chinese Academy of Sciences, Lanzhou 730000, China;
[2] University of Chinese Academy of Sciences, Beijing 100049, China

Abstract: Analysis of environmental significance and hydrochemical characteristics of river water in mountainous regions is vital for ensuring water security. In this study, we collected a total of 164 water samples in the western region of the Altay Mountains, China, in 2021. We used principal component analysis and enrichment factor analysis to examine the chemical properties and spatiotemporal variations of major ions (including F^-, Cl^-, NO_3^-, SO_4^{2-}, Li^+, Na^+, NH_4^+, K^+, Mg^{2+}, and Ca^{2+}) present in river water, as well as to identify the factors influencing these variations. Additionally, we assessed the suitability of river water for drinking and irrigation purposes based on the total dissolved solids, soluble sodium percentage, sodium adsorption ratio, and total hardness. Results revealed that river water had an alkaline aquatic environment with a mean pH value of 8.00. The mean ion concentration was ranked as follows: Ca^{2+}>SO_4^{2-}>Na^+>NO_3^->Mg^{2+}>K^+>Cl^->F^->NH_4^+>Li^+. Ca^{2+}, SO_4^{2-}, Na^+, and NO_3^- occupied 83% of the total ion concentration. In addition, compared with other seasons, the spatial variation of the ion concentration in spring was obvious. An analysis of the sources of major ions revealed that these ions originated mainly from carbonate dissolution and silicate weathering. The recharge impact of precipitation and snowmelt merely influenced the concentration of Cl^-, NO_3^-, SO_4^{2-}, Ca^{2+}, and Na^+. Overall, river water was in pristine condition in terms of quality and was suitable for both irrigation and drinking. This study provides a scientific basis for sustainable management of water quality in rivers of the Altay Mountains.

Keywords: environmental significance; hydrochemical characteristics; water quality; soluble sodium percentage (SSP); ion concentration; Altay Mountains

Citation: LIU Shuangshuang, WANG Feiteng, XU Chunhai, WANG Lin, LI Huilin. 2023. Environmental significance and hydrochemical characteristics of rivers in the western region of the Altay Mountains, China. Journal of Arid Land, 15(9): 1052–1066. https://doi.org/10.1007/s40333-023-0106-4

1 Introduction

Rivers, which support vital ecosystems, serve as crucial surface water resources that supply drinking water and irrigation water to the public (United Nations, 2019). In recent decades, the quality of river water has faced mounting pressures due to the impacts of human activities and climate-related stressors, leading to noticeable water environmental issues worldwide (Wen et al., 2015; He et al., 2020; Yapiyev et al., 2021). Consequently, there is an urgent requirement for continuous river monitoring to ensure sustainable management of water quality. The chemical

*Corresponding author: WANG Feiteng (E-mail: wangfeiteng@lzb.ac.cn)
Received 2023-02-21; revised 2023-05-21; accepted 2023-06-06

composition of river water is an essential indicator of water environmental quality, regional environmental characteristics, and the distribution and transformation of water components (Ye et al., 2010; Mapoma et al., 2016; Niu et al., 2017). Monitoring the chemical conditions of river water provides valuable insights into regional chemical weathering and key processes that govern hydrochemistry (Wang et al., 2015; Iqbal et al., 2018). Additionally, analyzing the chemical properties of river water aids in identifying the sources of major chemical constituents and understanding the evolution of geochemical solutes (Li et al., 2017; Pant et al., 2017).

Studies on the chemical status of runoff water have revealed the major contributors affecting river water quality, including atmospheric inputs, rock weathering, and human activities (Li et al., 2019). The solutes in river basins (particularly in the glacial catchments) predominantly originate from crustal mineral weathering (Li et al., 2022). Several qualitative and quantitative methods are used for assessing the physicochemical parameters and sources of solutes in river water. For instance, qualitative methods, such as Piper histograms (Piper, 1944), Gibbs scatter plots (Gibbs, 1970), factor analysis (Vermette et al., 1988; Okay et al., 2002; Li et al., 2014), and ionic ratios (Villegas et al., 2013), have been applied to identify the runoff water chemistry and mineral weathering. Quantitative methods, on the other hand, have been used to quantify the contribution of different solute sources based on chemical concentrations. For example, the forward model (Galy and France-Lanord, 1999) was utilized to determine the contribution of riverine solutes and could accurately assess the differences in the status of crustal mineral weathering (Yu et al., 2021).

Numerous previous studies have investigated the hydrochemistry of prominent rivers worldwide, including the Nile River (Dekov et al., 1997), Amazon River (Stallard and Edmond, 1983), and Ganges River–Yarlung Zangbo River (Galy and France-Lanord, 1999). In China, researches predominantly focused on hydrochemical characteristics of rivers originating from the Tibet Plateau (Li et al., 2019), Pamir Plateau (Wu et al., 2020), Qilian Mountains (Li et al., 2014), Tianshan Mountains (Yapiyev et al., 2021), and Altay Mountains (Liu et al., 2021). These researches have provided crucial insights into regional environmental changes, such as variations in the spatial and temporal distribution of river water chemistry (Jiang et al., 2015), as well as the sources of solutes in river water and the factors governing them (Li et al., 2019; Dong et al., 2022). Evaluating the hydrochemistry of rivers in these regions is vital for effective and sustainable management of water quality.

The western region of the Altay Mountains represents the northernmost concentration of modern glaciers in China (Wang et al., 2015). It not only serves as a representative arid region influenced by westerly circulation but also functions as a significant water source conservation area in northern Xinjiang Uygur Autonomous Region of China. In recent years, researchers have increasingly focused on water resources and environmental issues in the Altay Mountains, including river water chemistry (Liu et al., 2021), river water quantity (Zhang et al., 2010; Li et al., 2018), and soil-related concerns (Goenster-Jordan et al., 2021). However, studies on river water chemistry have typically relied on single-time-period sampling results to interpret concentration patterns, neglecting seasonal and annual variations (Liu et al., 2021). Furthermore, there is a lack of information on spatial patterns, such as the elevation distribution of ion concentration, due to scattered data and sampling discontinuities. The seasonal evolution and controlling factors of major ions in river water have not been systematically evaluated. To explore the hydrochemical characteristics and controlling factors in this region, researchers established the Altay Observation and Research Station for Cryospheric Science and Sustainable Development in the Altay Mountains in 2016. The primary objectives of this study were to: (1) analyze the spatiotemporal variability of major ions in river water, (2) determine the chemical weathering processes and the mechanisms underlying the seasonal evolution of river water in the study area, and (3) assess the suitability of river water for drinking and irrigation purposes.

2 Materials and methods

2.1 Study area

The western region of the Altay Mountains is mainly the origin area of the Burqin River (86°48′–88°36′E, 47°42′–49°12′N) and Haba River (85°31′–87°09′E, 47°38′–49°09′N; Fig. 1). The Burqin River is the largest tributary of the Ertix River, and the Burqin River Basin has a drainage area of approximately 8422.0 km^2, with an elevation of 470–4300 m. The glaciers in the Youyi Peak region (48°40′–49°10′N, 87°36′–87°53′E) supply water to the Burqin River Basin. The Haba River is the second largest tributary of the Ertix River. The drainage area of the Haba River Basin is approximately 7224.0 km^2. In 2020, the Altay Mountains contained 1927 glaciers with a total area of 1096.0 km^2 (Chang et al., 2022). The glaciers with an area of 0.1–0.5 km^2 (815 glaciers) account for 42% of the total number of glaciers (Chang et al., 2022). The Altay Mountains above 3000 m is mostly covered by glaciers and seasonal snow, which begin melting in June when the air temperatures are above 0.0°C (Qin et al., 2020). The landscapes are characterized by glaciers, snow, permafrost, forestlands, and grasslands from high to low elevations.

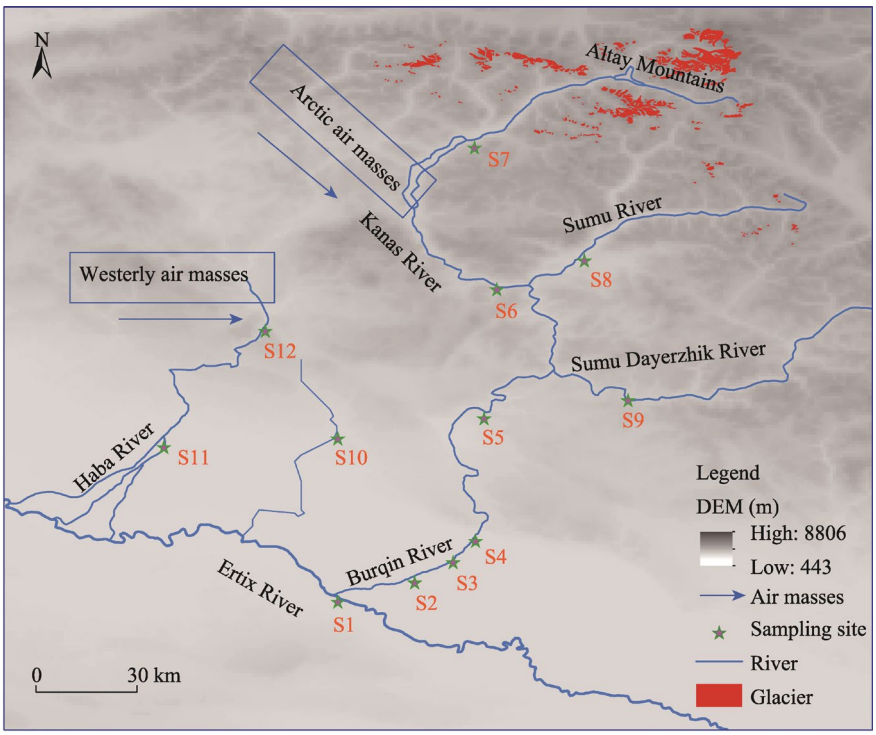

Fig. 1 Overview of the study area and distribution of the sampling sites. The Digital Elevation Model (DEM) is derived from www.earthdata.nasa.gov.

The entire region has a typical temperate continental climate (Liu et al., 2021). The local climate may also be influenced by westerlies and polar air masses. Besides, the annual average air temperature is 5.0°C, with a maximum temperature of 39.8°C occurring in July and a minimum temperature of –27.9°C occurring in December. The average annual precipitation is 159 mm. Precipitation occurs mainly due to water vapor transported by the westerly airflow throughout the year (Wang et al., 2015). These climatic characteristics are recorded by the meteorological station (86°87′E, 47°71′N; 483 m), which is situated about 5 km northeast of the confluence of the Burqin River and Ertix River. In addition to precipitation, glacier meltwater also supplies the region. The meltwater accounts for 45%–50% of all water sources (Lanzhou Institute of Glaciology and Geocryology, 1982).

2.2 Sample collection and measurement

In order to investigate hydrochemical characteristics of rivers in the western region of the Altay Mountains, we collected 164 samples from this region during January–December in 2021. Field sampling was conducted every 2 h from the 20th to the 21st of each month. The sampling sites are depicted in Figure 1. Firstly, empty sample bottles were washed by using a dilute HCl solution. After sampling, the collected samples were filtered using a 0.45-μm Millipore filter membrane. Subsequently, each sample was poured into two pre-washed polyethylene bottles. One of the bottles, which was used for cation analysis, was acidified using HNO_3 to a pH value below 2.00. The other bottle was used for anion and isotopic analyses. All samples were stored at a temperature of approximately 4.0°C before and during transportation to the laboratory for analyses in December 2021. Each sample was naturally thawed at normal room temperature (about 15.0°C) before being determined in the laboratory.

The hydrochemical analysis was conducted at the State Key Laboratory of Cryospheric Science of the Northwest Institute of Eco-Environment and Resources, Chinese Academy of Sciences. The pH was measured by a pH meter (PHSJ-4A, INESA Scientific Instrument Co., Ltd., Shanghai, China). We determined the total dissolved solids (TDS) and electrical conductivity (EC) based on a conductivity meter (DDSJ-308A, INESA Scientific Instrument Co., Ltd., Shanghai, China). The concentrations of cations (including Li^+, Na^+, NH_4^+, K^+, Mg^{2+}, and Ca^{2+}) were measured using an atomic absorption spectrometer (PE2380, Perkin Elmer, Massachusetts, USA), while those of anions (including F^-, Cl^-, NO_3^-, and SO_4^{2-}) were determined using an ion chromatography apparatus (Dionex100, Thermo Fisher Scientific, Massachusetts, USA). To ensure that the error between the analysis results of the water samples and those of the standard sample was less than 5%, we calibrated the apparatus after every 20 sample measurements.

2.3 Statistical methods

The principal component analysis (PCA) is a robust multivariate analysis method employed to identify the significant parameter variations within the data (Shrestha and Kazama, 2007; Wu et al., 2020). In this study, the PCA was utilized to condense several interconnected major ions (i.e., F^-, Cl^-, NO_3^-, SO_4^{2-}, Li^+, Na^+, NH_4^+, K^+, Mg^{2+}, and Ca^{2+}) into fewer uncorrelated variables, thereby facilitating subsequent analyses. The PCA algorithm was carried out in SPSS 19.0 software.

To assess the role of mineral weathering as the source of ions in this region, we calculated the enrichment factor (EF) using Ca^{2+} and Na^+ as the reference material. Ca^{2+} and Na^+ serve as the reference materials for soil and sea, respectively. The EF was calculated as follows:

$$EF_{soil} = [X / Ca^{2+}]_{water\ sample} / [X / Ca^{2+}]_{soil}, \quad (1)$$

$$EF_{sea} = [X / Na^{+}]_{water\ sample} / [X / Na^{+}]_{sea}, \quad (2)$$

where EF_{soil} is the enrichment factor for soil; X is the concentration of a specific ion (mg/L); $[X/Ca^{2+}]_{water\ sample}$ is the ratio of the concentration of a specific ion to the concentration of Ca^{2+} in the water samples; $[X/Ca^{2+}]_{soil}$ is the ratio of the concentration of a specific ion to the concentration of Ca^{2+} in soil (Okay et al., 2002); EF_{sea} is the enrichment factor for sea; $[X/Na^+]_{water\ sample}$ is the ratio of the concentration of a specific ion to the concentration of Na^+ in the water samples; $[X/Na^+]_{sea}$ is the ratio of the concentration of a specific ion to the concentration of Na^+ in sea (Keene et al., 1986); and Na^+ (mg/L) and Ca^{2+} (mg/L) represent the concentration of Na^+ and Ca^{2+}, respectively.

2.4 Suitability indices for drinking water and irrigation water

High concentration of Na^+ in irrigation water can lead to sodium hazards. Na^+ replaces both Ca^{2+} and Mg^{2+}, resulting in lower permeability and solid hardening (Shaki and Adeloye, 2006). In this study, we assessed the suitability of the water samples for irrigation based on the soluble sodium percentage (SSP; %) and sodium adsorption ratio (SAR) (Wu et al., 2020), which were calculated using the following equations:

$$SSP = \frac{Na^+}{Na^+ + K^+ + Ca^{2+} + Mg^{2+}} \times 100\%, \quad (3)$$

$$SAR = Na^+ \Big/ \sqrt{\left(Ca^{2+} + Mg^{2+}\right)/2}, \quad (4)$$

where K^+ (mg/L) and Mg^{2+} (mg/L) represent the concentration of K^+ and Mg^{2+}, respectively.

In addition, the total hardness (TH; mg/L), which refers to the combination of carbonate and non-carbonate hardness (Gao et al., 2017), was determined using the following equation:

$$TH = \left[Mg^{2+}/24 + Ca^{2+}/40\right] \times 100. \quad (5)$$

On the basis of the TH values, we classified the water samples into the following five classes: very soft water (TH≤75 mg/L), soft water (75 mg/L<TH≤150 mg/L), slightly hard water (150 mg/L<TH<300 mg/L), hard water (300 mg/L≤TH≤450 mg/L), and very hard water (TH>450 mg/L). We compared the TH values with those reported for the major rivers globally and the standard values derived from the World Health Organization (WHO, 2011), revealing the suitability of the water samples as drinking water.

3 Results and discussion

3.1 Hydrochemical characteristics and ion concentration

The pH, TDS, and ion concentration of the water samples are presented in Table 1. The pH values varied from 7.42 to 8.48, with a mean value of 8.00. The TDS ranged from 21.07 to 52.03 mg/L, with a mean value of 36.23 mg/L, suggesting an alkaline characteristic and low salinity. The mean ion concentration was ranked as follows: $Ca^{2+}>SO_4^{2-}>Na^+>NO_3^->Mg^{2+}>K^+>Cl^-$>$F^-$>$NH_4^+$>$Li^+$. Ca^{2+} alone contributed 42% of the total ion concentration, and SO_4^{2-}, Na^+, and NO_3^- accounted for 41% of the total ion concentration. The cation concentration was ranked as $Ca^{2+}>Mg^{2+}>Na^+>K^+$, which indicated that it is the same as the standard crustal material ($Ca^{2+}>Na^+>Mg^{2+}>K^+$).

Table 1 Hydrochemical characteristic and ion concentration of river water

Season	Item	pH	TDS (mg/L)	F^- (mg/L)	Cl^- (mg/L)	NO_3^- (mg/L)	SO_4^{2-} (mg/L)	Li^+ (mg/L)	Na^+ (mg/L)	NH_4^+ (mg/L)	K^+ (mg/L)	Mg^{2+} (mg/L)	Ca^{2+} (mg/L)
Spring	Mean	8.08	40.20	0.06	1.80	2.19	5.32	0.00	3.23	0.08	1.28	1.86	10.48
	SD	0.13	6.95	0.01	0.42	0.39	1.40	0.00	0.84	0.04	0.09	0.30	1.74
	Max	8.31	52.03	0.08	2.53	2.93	7.22	0.00	4.57	0.12	1.43	2.26	13.53
	Min	7.94	30.51	0.04	1.26	1.77	2.91	0.00	1.92	0.02	1.15	1.37	8.18
Summer	Mean	7.74	28.26	0.05	0.43	1.17	2.83	0.00	2.21	0.05	0.88	1.18	7.41
	SD	0.29	10.45	0.01	0.27	0.58	1.35	0.00	1.33	0.04	0.22	0.42	2.80
	Max	8.18	49.03	0.07	0.83	2.29	5.45	0.00	4.82	0.13	1.31	2.02	12.99
	Min	7.42	21.07	0.05	0.18	0.60	1.61	0.00	1.22	0.02	0.73	0.89	5.66
Autumn	Mean	7.94	34.99	0.81	0.48	1.32	4.30	0.00	2.69	0.04	1.05	1.49	9.36
	SD	0.14	5.82	0.83	0.13	0.28	0.75	0.00	0.75	0.02	0.12	0.13	1.59
	Max	8.10	46.35	1.84	0.72	1.81	5.36	0.01	4.16	0.06	1.27	1.72	12.50
	Min	7.71	30.37	0.06	0.33	0.99	3.09	0.00	2.01	0.01	0.94	1.35	8.24
Winter	Mean	8.22	41.50	0.09	0.95	1.71	6.19	0.00	3.63	0.16	1.09	1.73	11.06
	SD	0.19	5.51	0.02	0.63	0.05	2.72	0.00	1.48	0.06	0.17	0.10	1.18
	Max	8.48	51.88	0.13	2.17	1.80	11.55	0.00	6.54	0.24	1.41	1.83	13.29
	Min	8.00	35.63	0.07	0.40	1.64	3.94	0.00	2.42	0.09	0.93	1.54	9.88
Whole year	Mean	8.00	36.23	0.25	0.91	1.60	4.66	0.00	2.94	0.09	1.08	1.57	9.58
	SD	0.14	7.03	0.21	0.35	0.30	1.48	0.00	1.08	0.03	0.14	0.22	1.78
	Max	8.48	52.03	1.84	2.53	2.93	11.55	0.01	6.54	0.24	1.43	2.26	13.53
	Min	7.42	21.07	0.04	0.18	0.60	1.61	0.00	1.22	0.01	0.73	0.89	5.66

Note: TDS, total dissolved solids; Max, maximum; Min, minimum; SD, standard deviation.

Moreover, the anion concentration was ranked as SO_4^{2-}>NO_3^->Cl^-, which represented a difference compared to the standard seawater (Cl^->SO_4^{2-}>NO_3^-). In addition, the order of major anions and cations remained the same in different seasons, while the proportion of anions and cations varied. Specifically, Ca^{2+}, SO_4^{2-}, Na^+, and NO_3^- accounted for 81% of the total ion concentration in spring, the corresponding proportions in summer, autumn, and winter were 84%, 83%, and 85%, respectively. The result indicated that there are differences in the hydrochemical characteristics of river water in different seasons in the study area.

As depicted in Figure 2, the cations in the water samples were mainly concentrated in the lower right corner, indicating a dominance of Ca^{2+} in all seasons. Ca^{2+} accounted for 63% of the total cations. The proportion of Na^+ and K^+ in the total cations reached 26%, while the mean proportion of Mg^{2+} in the total cations was 10%. In contrast, the anions were characterized by the dominance of SO_4^{2-} (63%). NO_3^- and Cl^- accounted for 22% and 12% of the total anions, respectively. In general, the composition of cations and anions in most of the water samples exhibited minute differences across different seasons, demonstrating that the source of these ions was natural.

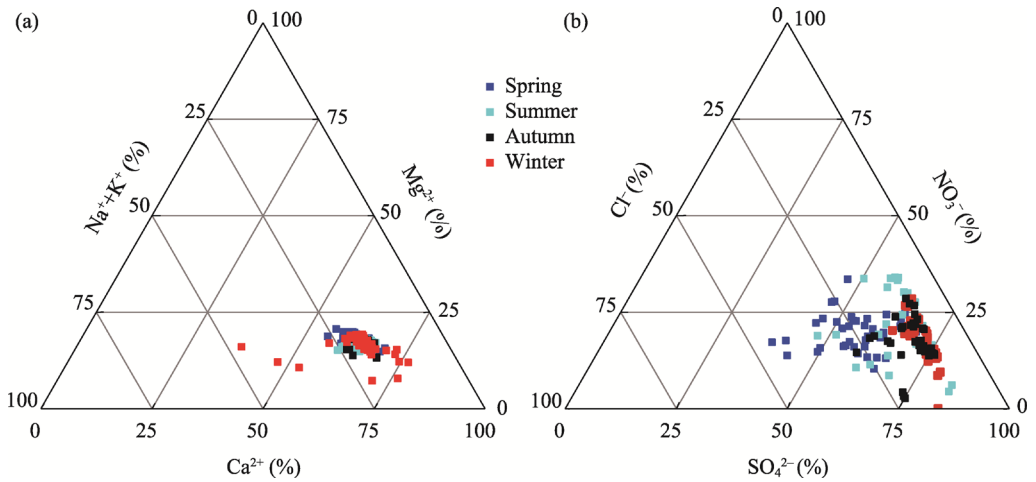

Fig. 2 Composition of cations (a) and anions (b) of river water

3.2 Spatiotemporal variation of the concentration of anions and cations

As shown in Figure 3, in spring, except for NH_4^+, the maximum mean concentration of all ions occurred at 484 m, while the minimum mean concentration of all ions occurred at 879 m. The maximum and minimum mean concentration of NH_4^+ was observed at 537 and 484 m, respectively. In summer, except for NH_4^+, the maximum mean concentration of all ions was observed at 879 m, while the minimum mean concentration of all ions mainly occurred at 484 m. In autumn, the maximum mean concentration of all ions occurred at 879 m, while the minimum mean concentration of all ions mainly occurred at 484 m. In winter, the maximum mean concentration of Ca^{2+}, Na^+, Mg^{2+}, K^+, NH_4^+, SO_4^{2-}, Cl^-, and F^- occurred at 879 m, while the minimum mean concentration of these ions was mainly observed at 484 m. In general, there were significant seasonal and spatial variations in the maximum mean concentration of most ions. Furthermore, the minimum mean concentration of most ions was found at 879 m in spring and 484 m in other seasons.

The temporal variations of the concentration of anions and cations of river water are illustrated in Figure 4. The concentration of Cl^-, NO_3^-, SO_4^{2-}, Na^+, Mg^{2+}, and Ca^{2+} was characterized by significant seasonal variations, with the maximum values observed in winter and the minimum values observed in late spring and summer. These ion concentrations varied from 0.35 to 12.51 mg/L, with a mean value of 3.07 mg/L. Moreover, the ion concentrations were higher in winter and early spring than in other seasons. This could be attributed to snowfall accumulation and low

runoff in these seasons. The ion concentrations decreased significantly in late spring and summer. This result indicated that snowmelt will recharge the river in spring, while precipitation will replenish the river in summer. Thus, the major ions in river water were diluted and the ion concentration was reduced.

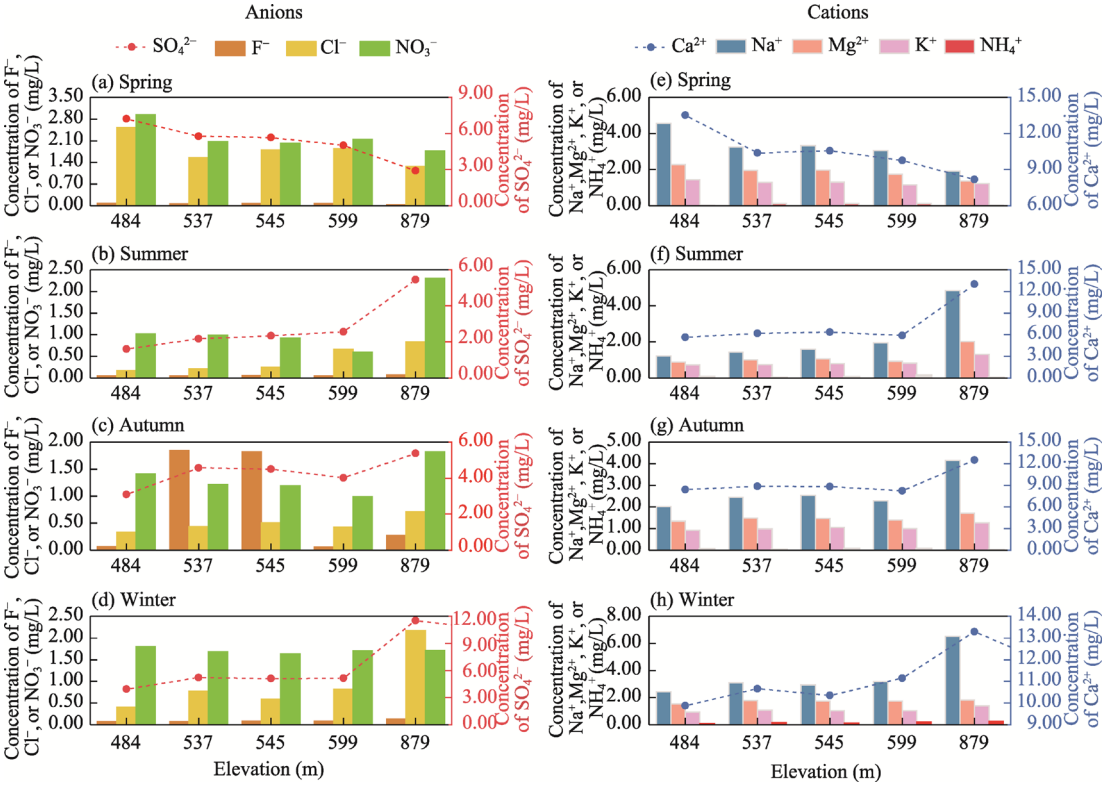

Fig. 3 Spatial variations of the concentration of anions (a–d) and cations (e–h) of river water in different seasons

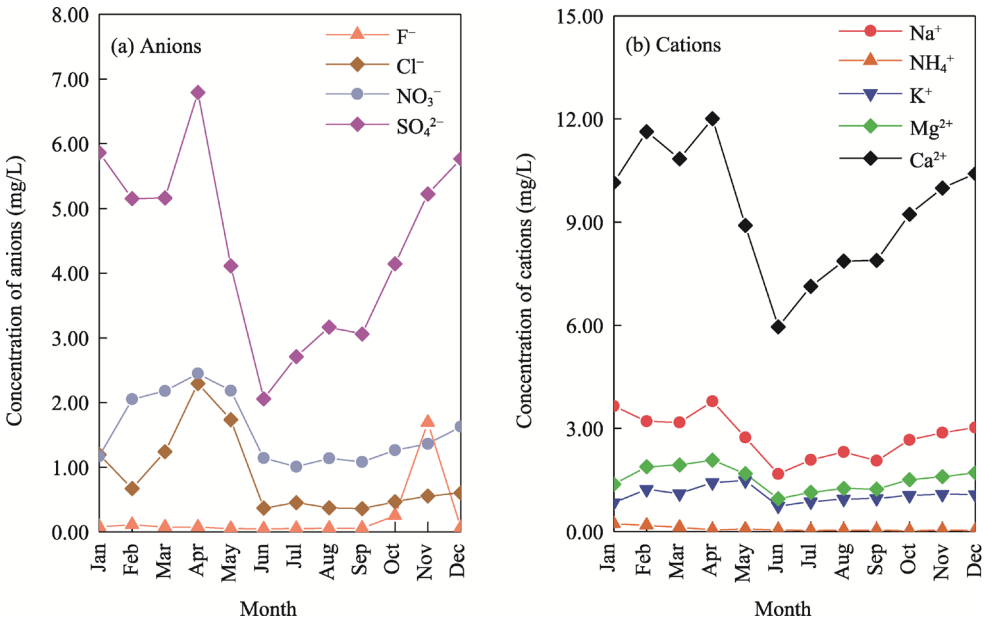

Fig. 4 Monthly variations of the concentration of anions (a) and cations (b) of river water

3.3 Correlations among pH, electrical conductivity (EC), and the concentration of anions and cations

Correlation analysis is a useful tool for examining the degree of dependence among different variables (Anshumali and Ramanathan, 2007). In this study, correlation analysis was performed to determine the relationships among pH, EC, and the concentration of anions and cations (Table 2). The positive correlation between pH and SO_4^{2-} indicated that river water is alkaline. The EC exhibited a significant positive relationship with all ions except for F^-. Moreover, the significant correlations of Ca^{2+} with NO_3^-, SO_4^{2-}, Cl^-, Na^+, K^+, and Mg^{2+} suggested that these ions come from a common source. No significant correlation was observed between F^- and other ions, indicating that F^- originated from different sources. The presence of Ca^{2+} and Mg^{2+} was primarily attributed to the dissolution of carbonates and evaporates. Similarly, the occurrence of SO_4^{2-} and Cl^- was predominantly linked to the dissolution of evaporates.

Table 2 Correlation coefficients of pH, electrical conductivity (EC), and the concentration of anions and cations of river water

	pH	EC	F^-	Cl^-	NO_3^-	SO_4^{2-}	Li^+	Na^+	NH_4^+	K^+	Mg^{2+}	Ca^{2+}
pH	1.000											
EC	0.070	1.000										
F^-	0.059	0.042	1.000									
Cl^-	0.115	0.637**	−0.052	1.000								
NO_3^-	0.056	0.792**	−0.049	0.590**	1.000							
SO_4^{2-}	0.203**	0.831**	0.104	0.711**	0.543**	1.000						
Li^+	−0.017	0.005	−0.020	−0.048	−0.051	0.013	1.000					
Na^+	0.145	0.883**	0.041	0.696**	0.593**	0.941**	−0.011	1.000				
NH_4^+	0.055	0.233**	−0.031	0.340**	0.013	0.398**	−0.061	0.388**	1.000			
K^+	−0.059	0.761**	0.013	0.657**	0.716**	0.604**	−0.016	0.630**	0.063	1.000		
Mg^{2+}	0.093	0.934**	0.061	0.611**	0.866**	0.742**	−0.016	0.755**	0.112	0.800**	1.000	
Ca^{2+}	0.199*	0.947**	0.046	0.536**	0.754**	0.742**	−0.007	0.782**	0.142	0.654**	0.892**	1.000

Note: ** indicates statistically significant correlation at $P<0.01$ level; * indicates statistically significant correlation at $P<0.05$ level.

In the PCA, three parameters with eigenvalues greater than 0.600 explained 98% of the total variance in the water samples (Table 3). The PC1 (principal component 1; 69%) presented a high load of most ions, except for F^- and NH_4^+, indicating a contribution from crustal sources (carbonates, evaporates, and sulfates). This was also confirmed by the positive correlations among Ca^{2+}, Li^+, Na^+, K^+, Mg^{2+}, Cl^-, SO_4^{2-}, and NO_3^- (Table 2). Furthermore, the PC2 (principal component 1) accounted for 15% of the total variance, with a high load of NH_4^+. NH_4^+ was strongly correlated with Cl^-, SO_4^{2-}, and Na^+, indicating the same source for these ions. The PC3 (principal component 3) explained 13% of the total variance, with a high load of F^-. The result suggested that F^- is mainly related to anthropogenic disturbances.

3.4 Sources of major ions in river water

To identify the possible sources of major ions, we conducted the enrichment factor analysis. Generally, the EF less than 1.00 indicates dilution compared to the reference material, while the EF greater than 1.00 indicates enrichment compared to the reference material (Zhang et al., 2007). Furthermore, when the EF is equal to 1.00, it indicates that there is no dilution or enrichment relative to the reference material. As depicted in Table 4, the EF_{soil} value of Na^+ was less than 1.00, indicating that the concentration of Na^+ is primarily influenced by sea. The EF_{soil} value of K^+ was lower than 1.00, while the EF_{sea} value of K^+ was greater than 15.00. The result suggested

Table 3 Principal component analysis of major ions of river water

Variable	PC1	PC2	PC3
F^-	–0.077	0.543	0.832
Cl^-	0.929	0.104	–0.346
NO_3^-	0.902	–0.413	–0.018
SO_4^{2-}	0.968	0.229	–0.081
Li^+	0.799	0.023	0.484
Na^+	0.977	0.067	–0.195
NH_4^+	–0.220	0.771	–0.568
K^+	0.979	0.151	0.002
Mg^{2+}	0.853	0.482	0.191
Ca^{2+}	0.993	0.072	–0.081
Explained variance (%)	68.958	15.427	13.334
Cumulative variance (%)	68.958	84.386	97.719

Note: PC1, PC2, and PC3 represent principal component 1, principal component 2, and principal component 3, respectively.

Table 4 Enrichment factor (EF) values of major ions of river water

Season	EF_{soil}						EF_{sea}						
	Na^+	K^+	Mg^{2+}	Cl^-	NO_3^-	SO_4^{2-}	K^+	Mg^{2+}	Ca^{2+}	F^-	Cl^-	NO_3^-	SO_4^{2-}
Spring	0.54	0.24	0.32	55.25	99.15	26.97	18.21	2.55	74.04	28.34	0.48	456.94	13.62
Summer	0.52	0.24	0.28	18.56	74.78	20.29	18.23	2.35	76.33	34.77	0.17	355.33	10.56
Autumn	0.50	0.22	0.28	16.67	67.21	24.46	17.94	2.44	79.31	435.29	0.16	331.84	13.23
Winter	0.58	0.20	0.28	27.72	29.77	29.77	13.80	2.09	69.36	34.55	0.23	317.15	14.08
Whole year	0.54	0.22	0.29	30.78	79.22	25.88	16.79	2.34	74.23	124.49	0.27	366.04	13.10

Note: EF_{soil} represents the enrichment factor for soil, and EF_{sea} represents the enrichment factor for sea.

that the concentration of K^+ is regulated by both sea and soil. The EF_{soil} value of Mg^{2+} was lower than 1.00, while its EF_{sea} value was higher than 1.00, suggesting that Mg^{2+} is derived from both soil and sea. The EF_{soil} value of Ca^{2+} ranged from 69.36 to 79.31, indicating that Ca^{2+} predominantly comes from soil. In addition, F^- was affected by soil, as evidenced by its EF_{soil} value. The EF_{sea} value of Cl^- was below 1.00, while its EF_{soil} value was higher than 10.00. This result demonstrated that the concentration of Cl^- is regulated by both sea and soil. Furthermore, NO_3^- was mainly affected by soil, with both EF_{soil} value and EF_{sea} value of NO_3^- above 1.00. SO_4^{2-} was mainly affected by soil, with an EF_{soil} exceeding 1.00. In addition, for all ions, differences were observed among different seasons.

3.5 Factors influencing hydrochemical characteristics of rivers

The hydrochemical characteristics of rivers can be influenced by various anthropogenic activities, such as increased grazing intensity, which has been known to modify water chemistry in recent years (Goenster-Jordan et al., 2021). Additionally, it has been reported that the growth of tourism and local agricultural practices have the potential to alter natural water chemistry (Negrel et al., 1993). Therefore, in order to assess the impact of rock weathering and human activities on water quality, we calculated the ratios of NO_3^-, SO_4^{2-}, and CI^- to Na^+ according to Gaillardet et al. (1999a, b). Figure 5 illustrates that no significant correlation was observed between the ratio of NO_3^- to Na^+ (NO_3^-/Na^+) and the ratio of SO_4^{2-} to Na^+ (SO_4^{2-}/Na^+) in different seasons, suggesting that the sources of these ions were different. Most of the NO_3^-/Na^+ values were below 0.8, indicating a minimal contribution from human activities.

Furthermore, we drew the Gibbs diagram based on the ratio of Na^+ to Na^+ and Ca^{2+} ($Na^+/(Na^+ + Ca^{2+})$). The TDS content was employed to identify the predominant factors influencing

hydrochemical characteristics of rivers such as precipitation dominance, weathering dominance, or evaporation-crystallization dominance. As shown in Figure 6, most of the water samples had moderate TDS and low $Na^+/(Na^+{+}Ca^{2+})$ values, indicating that rock weathering was the leading process regulated hydrochemical characteristics of rivers. To distinguish the main rocks (i.e., carbonates, evaporates, and sulfates), we calculated the ratio of Ca^{2+} to Na^+ (Ca^{2+}/Na^+) and the ratio of Mg^{2+} to Na^+ (Mg^{2+}/Na^+). The majority of the water samples were found to lie between carbonate dissolution and silicate weathering, indicating that both processes contribute significantly to the hydrochemical characteristics of rivers.

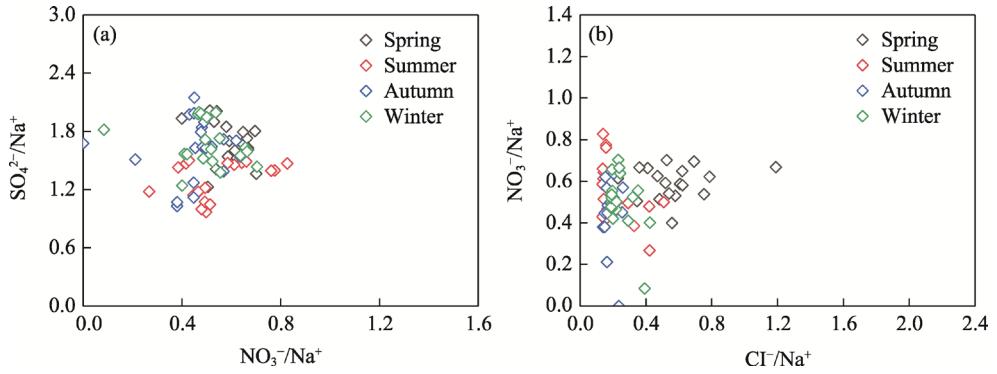

Fig. 5 (a), relationship between the ratio of NO_3^- to Na^+ (NO_3^-/Na^+) and the ratio of SO_4^{2-} to Na^+ (SO_4^{2-}/Na^+); (b), relationship between the ratio of Cl^- to Na^+ (Cl^-/Na^+) and NO_3^-/Na^+

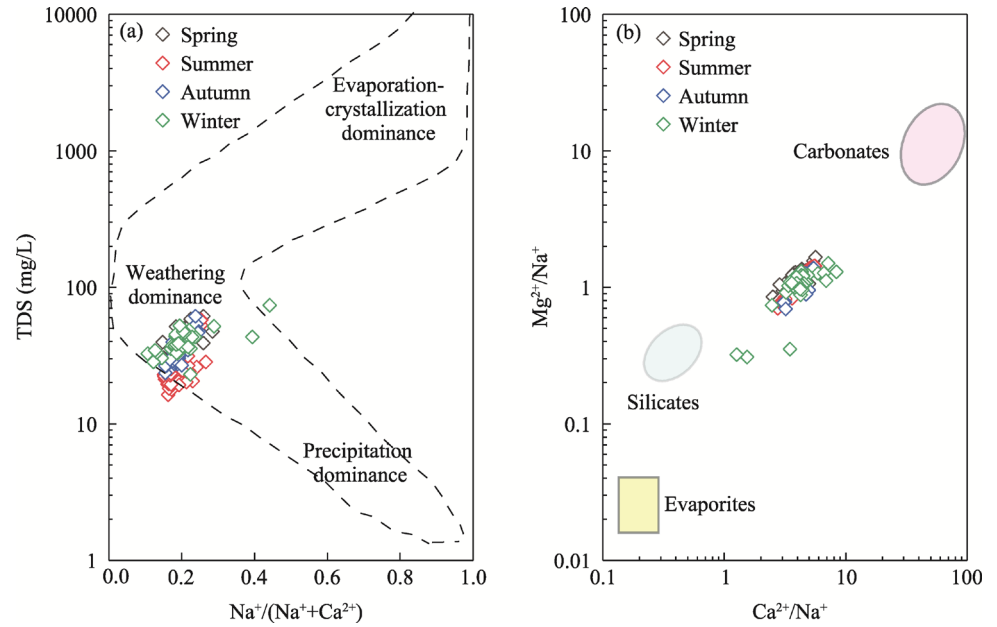

Fig. 6 Influencing factors for hydrochemical characteristics showed by Gibbs diagram. (a), Gibbs diagram of the ratio of Na^+ to Na^+ and Ca^{2+} ($Na^+/(Na^+{+}Ca^{2+})$) to total dissolved solids (TDS); (b), relationship between the ratio of Ca^{2+} to Na^+ (Ca^{2+}/Na^+) and the ratio of Mg^{2+} to Na^+ (Mg^{2+}/Na^+).

The main ions of water river in the western region of the Altay Mountains were Ca^{2+}, Mg^{2+}, and SO_4^{2-} (Fig. 2). However, significant differences in ion concentration were observed as the elevation gradient changed (Fig. 3). At low elevations (<500 m), Ca^{2+} and Cl^- were the dominant ions; while, at high elevations (from 500 to 900 m), Ca^{2+} and SO_4^{2-} were the dominant ions. A related study observed that the vertical distribution of major ions can provide insights into the vertical distribution of rock formations (Li et al., 2018). The maximum values of K^+, NH_4^+, F^-, Li^+, and Mg^{2+} remained consistent across different seasons, suggesting that the concentrations of

these ions were minimally affected by precipitation and meltwater recharge. The maximum values of Cl^-, NO_3^-, SO_4^{2-}, Ca^{2+}, and Na^+ first decreased and then increased from spring to winter. The result indicated that the concentrations of Cl^-, NO_3^-, SO_4^{2-}, Ca^{2+}, and Na^+ are affected by the recharge effects of precipitation and meltwater. However, the recharge effects of precipitation and meltwater on K^+, NH_4^+, F^-, Li^+, and Mg^{2+} were minimal.

3.6 Comparison of hydrochemical characteristics between the study area and other mountains

The hydrochemical characteristics of the study area are consistent with those of other mountains (Table 5). For instance, the pH values of the Ertix River and Ulungur River were also alkaline, with a small range of variation. These rivers contained abundant Ca^{2+}, Na^+, HCO_3^-, and SO_4^{2-}, which are the most common cations and anions (Liu et al., 2021). Additionally, the average TDS in the Ertix River and Ulungu River is reported to be significantly higher than that in the western region of the Altay Mountains, which may be attributed to the comprehensive impact of geological conditions, supply sources, climatic factors, and human activities (Zabaleta et al., 2007). The hydrochemical characteristics of the Burqin River and Haba River were related to the weathering of carbonates and silicates. In contrast, it has been reported that the ion composition of the Ertix River and Ulungu River is influenced by various factors, including carbonates dissolution, silicates weathering, and evaporates dissolution (Liu et al., 2021).

Table 5 Comparison of hydrochemical characteristics between the western region of the Altay Mountains and other mountains

Region	River	pH	TDS (mg/L)	Cl^- (mg/L)	NO_3^- (mg/L)	SO_4^{2-} (mg/L)	HCO_3^- (mg/L)	Na^+ (mg/L)	K^+ (mg/L)	Mg^{2+} (mg/L)	Ca^{2+} (mg/L)	Reference
Altay Mountains	Burqin River and Haba River	8.00	36.20	0.91	1.60	4.66	-	2.94	1.08	1.57	9.58	This study
	Ertix River and Ulungur River	7.80	126.00	7.06	-	35.00	65.70	12.60	1.50	4.26	32.40	Liu et al. (2021)
Tianshan Mountains	Source region of Syr Darya River	8.20	291.40	3.00	3.50	45.00	200.00	5.00	1.44	11.00	35.00	Ma et al. (2019)
	Kax River	8.00	239.20	1.70	-	22.55	120.80	4.10	1.67	5.83	39.38	Feng et al. (2022)
	Bortala River	8.50	246.00	14.30	-	67.50	157.00	21.40	2.32	7.83	52.80	Liu et al. (2021)
Qilian Mountains	Hulugou River	-	-	16.60	2.67	360.05	-	82.67	2.29	33.70	88.21	Li et al. (2014)
	Shule River	8.50	160.10	8.20	-	23.70	88.70	12.60	0.90	10.40	14.80	Qu et al. (2019)
Central Tibetan Plateau	Source region of Yangtze River	7.60	778.00	233.70	1.30	114.90	188.50	157.70	5.50	22.90	53.40	Jiang et al. (2015)
	Zhajia Tsangpo River	9.10	947.00	394.81	2.62	164.11	55.20	245.00	12.20	27.30	45.50	Qu et al. (2019)
Southern and northern parts of the Tibetan Plateau	Yellow River	8.40	609.50	22.90	-	49.40	389.50	33.30	2.10	33.70	75.80	Qu et al. (2019)
	Heihe River	8.70	462.00	8.20	2.20	80.40	263.30	15.70	1.70	30.40	60.00	Qu et al. (2019)
	Nujiang River	8.40	141.00	5.00	0.00	31.00	66.00	3.00	1.00	7.00	24.00	Huang et al. (2009)
	Yarlung Zangbo River	8.80	117.30	2.40	1.00	37.40	74.10	5.70	1.00	5.10	27.90	Qu et al. (2017)

Note: -, no data.

The ion concentration of river water in the western region of the Altay Mountains was far lower than that in other mountains, which is attributed to the different and unique lithology and geographic conditions of these mountains (Table 5). For instance, the mean concentration of Cl^- in the study area was 0.91 mg/L, which is lower than that reported in other mountains. The TDS of the study area was also relatively low, due to lower Ca^{2+} and SO_4^{2-}. The mean concentrations of Ca^{2+} and SO_4^{2-} were 9.58 and 4.66 mg/L, respectively, which are more than 17 times lower than those in other rivers. In addition, the high concentrations of Ca^{2+}, HCO_3^-, and SO_4^{2-} in the rivers of the Tianshan Mountains demonstrated that hydrochemical characteristics are mainly affected by carbonate dissolution and silicate weathering (Ma et al., 2019; Liu et al., 2021; Feng and Yang, 2022). High concentrations of Ca^{2+}, Mg^{2+}, and HCO_3^- in rivers in southern and

northern parts of the Tibetan Plateau were also affected by carbonate dissolution and silicate weathering (Huang et al., 2009; Qu et al., 2017, 2019). However, high concentrations of Na^+, Cl^-, and SO_4^{2-} in rivers of central Tibetan Plateau were controlled by evaporates dissolution (Galy and France-Lanord, 1999). Furthermore, high concentrations of Ca^{2+}, Mg^{2+}, and SO_4^{2-} in the Hulugou River of the Qilian Mountains were affected by the weathering and dissolution of dolomite (Li et al., 2014). However, it is reported that in the Shule River of the Qilian Mountains, the ion composition (Ca^{2+}, Mg^{2+}, and HCO_3^-) is mainly influenced by the weathering of carbonate and silicate (Qu et al., 2019).

3.7 Impacts on the suitability of river water for drinking and irrigation

Glaciers and snowmelt in the Altay Mountains are important water resources for residents and economic development of this region (Wang et al., 2015). However, due to the high sensitivity of small glaciers in the Altay Mountains, the lack of water may threaten this region. Therefore, considering the impact of water scarcity on human and ecosystem health, we conducted an assessment of river water quality. In accordance with the guidelines of the World Health Organization, we found that the TDS and ion concentrations in the study area were considerably below the maximum limits for drinking water (WHO, 2011). The water quality of this study area is similar to that of the Indus River and Ganges River–Yarlung Zangbo River (Qu et al., 2019). Furthermore, all water samples were very soft water, indicating that the water is safe to drink (Fig. 7).

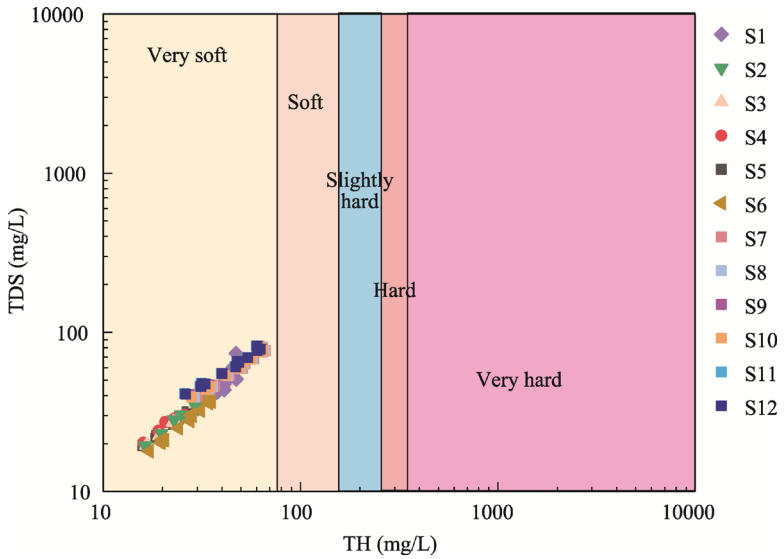

Fig. 7 River water quality at different sampling sites in the western region of the Altay Mountains. TH represent the total hardness. S1 to S12 represent 12 sampling sites, and the locations of these sites are depicted in Figure 1.

We also assessed the suitability of river water for irrigation (Table 6). The mean SSP value in the region was 18% (±4%) (Table 6), indicating excellent irrigation quality. Moreover, compared to other sampling sites, the SSP of S1 (Site 1) was relatively high, which may be related to human activities in the downstream region. In this study, most of the SPP values (81%) achieved excellent irrigation water quality. Similarly, the mean SAR value was 1.2 (±0.5), and the irrigation water quality at all sampling sites was excellent (Table 6). Overall, river water in the western region of the Altay Mountains is safe for drinking and irrigation.

We evaluated the suitability of river water for drinking and irrigation based on the TDS, TH, SSP, and SAR of the water samples. Future studies could also focus on comprehensive long-term field observations of water chemistry and isotopes in glacial areas. This will facilitate the systematic assessment of water quality and hydrochemical characteristics in headwater catchments, particularly in data-poor regions, such as the Altay Mountains.

Table 6 Soluble sodium percentage (SSP) and sodium adsorption ratio (SAR) of river water in the western region of the Altay Mountains

Sampling site	SSP (%)	SAR	Sampling site	SSP (%)	SAR
S1	21±5	1.7	S7	18±6	1.1
S2	18±2	1.1	S8	17±3	1.0
S3	17±2	1.1	S9	20±3	1.3
S4	19±3	1.2	S10	16±3	0.9
S5	16±4	0.9	S11	18±6	1.0
S6	22±2	1.7	S12	18±3	1.2

Note: Mean±SD.

4 Conclusions

In this study, the mean ion concentration was ranked as follows: $Ca^{2+}>SO_4^{2-}>Na^+>NO_3^-$>$Mg^{2+}>K^+>Cl^->F^->NH_4^+>Li^+$. Among these ions, Ca^{2+}, SO_4^{2-}, Na^+, and NO_3^- accounted for 83% of the total ion concentration. The spatial variation of ion concentration exhibited greater stability in summer, autumn, and winter. Results of Gibbs diagram showed that river water chemistry was primarily influenced by carbonate dissolution and silicate weathering. There were differences in hydrochemical characteristics at different elevations, with low elevations dominated by Ca^{2+} and Cl^-, while high elevations dominated by Ca^{2+} and SO_4^{2-}. In addition, the recharge effects of precipitation and snowmelt primarily affected the concentrations of Cl^-, NO_3^-, SO_4^{2-}, Ca^{2+}, and Na^+. The suitability evaluation of river water revealed that river water is safe for drinking and irrigation. Nonetheless, this study is only a preliminary investigation, and follow-up researches may focus on further strengthening the field monitoring of water chemistry and isotopes in the glacial region of the Altay Mountains.

Conflict of interest

The authors declare that they have no known competing financial interests or personal relationships that could have appeared to influence the work reported in this paper.

Acknowledgements

This research was supported by the State Key Laboratory of Cryospheric Science of China (SKLCS-ZZ-2022), the National Key Research and Development Research and Development Program of China (2020YFF0304400), and the Third Scientific Expedition in Xinjiang Uygur Autonomous Region of China (2022xjkk0701).

Author contributions

Conceptualization: LIU Shuangshuang; Data curation: LIU Shuangshuang; Methodology: XU Chunhai; Investigation: WANG Lin; Formal analysis: LIU Shuangshuang; Writing - original draft preparation: LIU Shuangshuang; Writing - review and editing: LIU Shuangshuang; Funding acquisition: WANG Feiteng; Resources: WANG Feiteng; Supervision: WANG Feiteng; Project administration: WANG Feiteng; Software: LI Huilin; Validation: LI Huilin; Visualization: XU Chunhai.

References

Anshumali, Ramanathan A L. 2007. Seasonal variation in the major ion chemistry of Pandoh lake, Mandi district, Himachal Pradesh, India. Applied Geochemistry, 22(8): 1736–1747.

Chang J W, Wang N L, Li Z J, et al. 2022. Accelerated shrinkage of glaciers in the Altai Mountains from 2000 to 2020. Frontiers in Earth Science, 10: 919051, doi: 10.3389/feart.2022.919051.

Dekov V M, Komy Z, Araújo F, et al. 1997. Chemical composition of sediments, suspended matter, river water and ground water of the Nile (Aswan-Sohag traverse). Science of The Total Environment, 201(3): 195–210.

Dong X Y, Zhao L J, Wang N L, et al. 2022. Spatial variations on the hydrochemistry, controls, and solute sources of surface water in the Weihe River Basin, China. Environmental Science and Pollution Research, 29(38): 57790–57807.

Feng X C, Yang Y H. 2022. Hydrochemical and stable isotopic spatiotemporal variation characteristics and their environmental significance in the Kashi River Mountain Area of Ili, Xinjiang, China. Environmental Geochemistry and Health, 44(3): 799–816.

Gaillardet J, Dupré B, Allègre C J. 1999a. Geochemistry of large river suspended sediments: Silicate weathering or recycling tracer? Geochimica et Cosmochimica Acta, 63(23–24): 4037–4051.

Gaillardet J, Dupré B, Louvat P, et al. 1999b. Global silicate weathering and CO_2 consumption rates deduced from the chemistry of large rivers. Chemical Geology, 159(1–4): 3–30.

Galy A, France-Lanord C. 1999. Weathering processes in the Ganges-Brahmaputra basin and the riverine alkalinity budget. Chemical Geology, 159(1–4): 31–60.

Gao Z Y, Lin Z J, Niu F J, et al. 2017. Hydrochemistry and controlling mechanism of lakes in permafrost regions along the Qinghai-Tibet Engineering Corridor, China. Geomorphology, 297: 159–169.

Gibbs R J. 1970. Mechanisms controlling world water chemistry. Science, 170(3962): 1088–1090.

Goenster-Jordan S, Ingold M, Jannoura R, et al. 2021. Soil microbial properties of subalpine steppe soils at different grazing intensities in the Chinese Altai Mountains. Scientific Reports, 11: 1653, doi: 10.1038/s41598–021–81120-y.

He J, Wu X, Zhang Y, et al. 2020. Management of water quality targets based on river-lake water quality response relationships for lake basins-A case study of Dianchi Lake. Environmental Research, 186: 109479, doi: 10.1016/j.envres.2020.109479.

Huang X, Sillanpaa M, Gjessing E T, et al. 2009. Water quality in the Tibetan Plateau: Major ions and trace elements in the headwaters of four major Asian rivers. Science of The Total Environment, 407(24): 6242–6254.

Iqbal J, Nazzal Y, Howari F, et al. 2018. Hydrochemical processes determining the groundwater quality for irrigation use in an arid environment: the case of Liwa aquifer, Abu Dhabi, United Arab Emirates. Groundwater for Sustainable Development, 7: 212–219.

Jiang L G, Yao Z J, Liu Z F, et al. 2015. Hydrochemistry and its controlling factors of rivers in the source region of the Yangtze River on the Tibetan Plateau. Journal of Geochemical Exploration, 155: 76–83.

Keene W C, Pszenny A A P, Galloway J N, et al. 1986. Sea-salt corrections and interpretation of constituent ratios in marine precipitation. Journal of the Geothermal Research-Atmospheres, 91(D6): 6647–6658.

Li Q, Yang T, Qi Z M, et al. 2018. Spatiotemporal variation of snowfall to precipitation ratio and its implication on water resources by a regional climate model over Xinjiang, China. Water, 10(10): 1463, doi: 10.3390/w10101463.

Li X Y, Ding Y J, Han T D, et al. 2019. Seasonal controls of meltwater runoff chemistry and chemical weathering at Urumqi Glacier No.1 in central Asia. Hydrological Processes, 33(26): 3258–3281.

Li X Y, Wang N L, Ding Y J, et al. 2022. Globally elevated chemical weathering rates beneath glaciers. Nature Communications, 13(1): 407, doi: 10.1038/s41467-022-28032-1.

Li Z, Xiao J, Evaristo J, et al. 2019. Spatiotemporal variations in the hydrochemical characteristics and controlling factors of streamflow and groundwater in the Wei River of China. Environmental Pollution, 254: 113006, doi: 10.1016/j.envpol.2019.113006.

Li Z J, Song L L, Ma J Z. 2017. Hydrochemical characteristics and environmental significance in different ablation period in Hulugou river basin in Qilian Mountain. Environmental Earth Sciences, 76(17): 606, doi: 10.1007/s12665-017-6911-3.

Li Z J, Li Z X, Song L L, et al. 2018. Environment significance and hydrochemical characteristics of supra-permafrost water in the source region of the Yangtze River. Science of The Total Environment, 644: 1141–1151.

Li Z X, Feng Q, Liu W, et al. 2014. Study on the contribution of cryosphere to runoff in the cold alpine basin: A case study of Hulugou River Basin in the Qilian Mountains. Global and Planetary Change, 122: 345–361.

Liu C H, Shi Y F, Wang Z T, et al. 2018. Glacier Inventory of China (II): Altay Mountains. Beijing: Science Press.

Liu W, Ma L, Abuduwaili J. 2021. Water quality for agricultural irrigation and aquatic arsenic health risk in the Altay and Tianshan mountains, Central Asia. Agronomy-Basel, 11(11): 2270, doi: 10.3390/agronomy11112270.

Ma L, Abuduwaili J, Li Y M, et al. 2019. Hydrochemical characteristics and water quality assessment for the upper reaches of Syr Darya River in Aral Sea Basin, Central Asia. Water, 11(9): 1893, doi: 10.3390/w11091893.

Mapoma H W T, Xie X J, Zhang L P, et al. 2016. Hydrochemical characteristics of rural community groundwater supply in Blantyre, Southern Malawi. Journal of African Earth Sciences, 114: 192–202.

Negrel P, Allegre C J, Dupre B, et al. 1993. Erosion sources determined by inversion of major and trace-element ratios and strontium isotopic-ratios in river water-the Congo Basin case. Earth and Planetary Science Letters, 120(1–2): 59–76.

Niu H W, Kang S C, Shi X F, et al. 2017. Water-soluble elements in snow and ice on Mt. Yulong. Science of The Total Environment, 574: 889–900.

Okay C, Akkoyunlu B O, Tayanc M. 2002. Composition of wet deposition in Kaynarca, Turkey. Environmental Pollution, 118(3): 401–410.

Pant R R, Zhang F, Rehman F U, et al. 2017. Spatiotemporal variations of hydrogeochemistry and its controlling factors in the Gandaki river basin, central Himalaya Nepal. Science of The Total Environment, 770: 622–623.

Piper A M. 1944. A graphic procedure in the geochemical interpretation of water-analyses. Transactions-American Geophysical Union, 25: 914–923.

Qin J, Wu J K, Han T D, et al. 2020. Quantitatively estimate the components of natural runoff and identify the impacting factors in a snow-fed river basin of China. Sciences in Cold and Arid Regions, 12(3): 154–164.

Qu B, Zhang Y L, Kang S C, et al. 2017. Water chemistry of the southern Tibetan Plateau: an assessment of the Yarlung Tsangpo river basin. Environmental Earth Sciences, 76(2): 74, doi: 10.1007/s12665-017-6393-3.

Qu B, Zhang Y L, Kang S C, et al. 2019. Water quality in the Tibetan Plateau: Major ions and trace elements in rivers of the "Water Tower of Asia". Science of The Total Environment, 649: 571–581.

Shaki A A, Adeloye A J. 2006. Evaluation of quantity and quality of irrigation water at Gadowa irrigation project in Murzuq basin, southwest Libya. Agricultural Water Resources Management, 84(1–2): 193–201.

Shrestha S, Kazama F. 2007. Assessment of surface water quality using multivariate statistical techniques: A case study of the Fuji river basin, Japan. Environmental Modelling & Software, 22(4): 464–475.

Stallard R F, Edmond J M. 1983. Geochemistry of the Amazon: 2. The influence of geology and weathering environment on the dissolved load. Journal of Geophysical Research Oceans, 88(C14): 9671–9688.

United Nations. 2019. Goal 6: Ensure Availability and Sustainable Management of Water and Sanitation for All. [2023-01-21]. https://sustainabledevelopment.un.org/sdg6.

Vermette S J, Drake J J, Landsberger S. 1988. Intra-urban precipitation quality: Hamilton, Canada. Water, Air, and Soil Pollution, 38: 37–53.

Villegas P, Paredes V, Betancur T, et al. 2013. Assessing the hydrochemistry of the Uraba Aquifer, Colombia by principal component analysis. Journal of Geochemical Exploration, 134: 120–129.

Wang J L, Jin M G, Jia B J, et al. 2015. Hydrochemical characteristics and geothermometry applications of thermal groundwater in northern Jinan, Shandong, China. Geothermics, 57: 185–195.

Wang P Y, Li Z Q, Luo S F, et al. 2015. Five decades of changes in the glaciers on the Friendship Peak in the Altai Mountains, China: Changes in area and ice surface elevation. Cold Regions Science and Technology, 116: 24–31.

Wen Y, Schoups G, Nick V D G. 2015. Population and Climate Pressures on Global River Water Quality. EGU General Assembly Conference Abstracts. [2023-01-21]. https://ui.adsabs.harvard.edu/abs/2015EGUGA..17.7614W/abstract.

WHO. 2011. Guidelines for Drinking-Water Quality. [2023-01-21]. https://www.who.int/publications/i/item/9789241549950.

Wu H W, Wu J L, Li J, et al. 2020. Spatial variations of hydrochemistry and stable isotopes in mountainous river water from the Central Asian headwaters of the Tajikistan Pamirs. CATENA, 193: 104639, doi: 10.1016/j.catena.2020.104639.

Yapiyev V, Wade A J, Shahgedanova M, et al. 2021. The hydrochemistry and water quality of glacierized catchments in Central Asia: A review of the current status and anticipated change. Journal of Hydrology-Regional Studies, 38: 100960, doi: 10.1016/j.ejrh.2021.100960.

Ye H M, Yuan X Y, Ge M X, et al. 2010. Water chemistry characteristics and controlling factors in the northern rivers in the Taihu Basin. Energy Ecology and Environment, 19(1): 23–27. (in Chinese)

Yu Z L, Wu G J, Li F, et al. 2021. Glaciation enhanced chemical weathering in a cold glacial catchment, western Nyaingentanglha Mountains, central Tibetan Plateau. Journal of Hydrology, 597: 126197, doi: 10.1016/j.jhydrol.2021.126197.

Zabaleta A, Martinez M, Uriarte J A, et al. 2007. Factors controlling suspended sediment yield during runoff events in small headwater catchments of the Basque Country. CATENA, 71(1): 179–190.

Zhang G X, Sun S F, Ma Y F, et al. 2010. The response of annual runoff to the height change of the summertime 0°C level over Xinjiang. Journal of Geographical Sciences, 20(6): 833–847.

Zhang M Y, Wang S J, Wu F C, et al. 2007. Chemical compositions of wet precipitation and anthropogenic influences at a developing urban site in southeastern China. Atmospheric Research, 84(4): 311–322.